CrossMark

RESEARCH PAPER

Isonitrile-functionalized ruthenium nanoparticles: intraparticle charge delocalization through Ru=C=N interfacial bonds

Fengqi Zhang · Lin Huang · Jiasui Zou · Jun Yang · Xiongwu Kang ⓘ · Shaowei Chen

Abstract Ruthenium nanoparticles (2.06 ± 0.46 nm in diameter) stabilized by 1-hexyl-4-isocyanobenzene (CNBH), denoted as RuCNBH, were prepared by the self-assembly of isonitrile molecules onto the surface of "bare" Ru colloids by virtue of the formation of Ru=C=N− interfacial bonds. FTIR measurements showed that the stretching vibration of the terminal −N≡C bonds at 2119 cm^{-1} for the monomeric ligands disappeared and concurrently three new bands at 2115, 2043, and 1944 cm^{-1} emerged with RuCNBH nanoparticles, which was ascribed to the transformation of −N≡C to Ru=C=N− by back donation of Ru-d electrons to the π* orbital of the organic ligands. Metathesis reaction of RuCNBH with vinyl derivatives further corroborated the nature of the Ru=C interfacial bonds. When 1-isocyanopyrene (CNPy) was bounded onto the Ru nanoparticles surface through Ru=C=N interfacial bond (denoted as RuCNPy), the emission maximum was found to red-shift by 27 nm, as compared to that of the CNPy monomers, along with a reduced fluorescence lifetime, due to intraparticle charge delocalization that arose from the conjugated Ru=C=N− interfacial bonds. The results of this study further underline the significance of metal−organic interfacial bonds in the control of intraparticle charge-transfer dynamics and the optical and electronic properties of metal nanoparticles.

F. Zhang · L. Huang · J. Zou · J. Yang · X. Kang (✉) ·
S. Chen (✉)
New Energy Research Institute, School of Environment and Energy, Guangzhou Higher Education Mega Centre, South China University of Technology, Guangzhou 510006, China
e-mail: esxkang@scut.edu.cn
e-mail: shaowei@ucsc.edu

F. Zhang · L. Huang · J. Zou · J. Yang · X. Kang · S. Chen
Guangzhou Higher Education Mega Centre, Guangzhou 510006, China

S. Chen
Department of Chemistry and Biochemistry, University of California, 1156 High Street, Santa Cruz, CA 95064, USA

Introduction

Noble metal nanoparticles passivated with organic monolayers, due to their unique optical and electronic properties, have found diverse applications in, for instance, molecular electronics, chemical sensing, and catalysis.(Lu and Chen 2012) In order to stabilize the nanoparticles and further manipulate the materials properties, surface functionalization with organic molecules has been utilized as a powerful tool. Among these, mercapto-derivatives, due to the strong affinity of thiol groups to transition metal surfaces, have been used as the ligands of choice for the surface passivation of metal nanoparticles (Chen et al. 1998). Lately, formation of metal-carbon and metal-

nitrogen covalent bonds has been demonstrated as an effective tool in the regulation of the optical and electronic properties of metal nanoparticles due to the formation of metal-carbon/nitrogen covalent bonds at the metal-ligand interface (Kang et al. 2012a; Kang et al. 2010; Kang et al. 2012b). For instance, intraparticle charge delocalization has been observed in ruthenium nanoparticles functionalized with conjugated metal-carbon covalent bonds, such as ruthenium-carbene (Ru=C) bonds (Chen et al. 2006), ruthenium-vinylidene (Ru=C=CH–) bonds (Kang et al. 2012b), and ruthenium-nitrene (Ru=N) bonds (Kang et al. 2012a). Very recently, we show that Ru nanoparticles might also be passivated with nitrile ligands by the formation of Ru–N≡interfacial linkages (Zhang et al. 2017). In these systems, the electrochemical and spectroscopic characteristics of the nanoparticle-bound organic ligands are analogous to those of their dimeric counterparts with a conjugated spacer. Because of the formation of $d\pi$-$p\pi$ interactions between the transition-metal nanoparticles and terminal carbon or nitrogen moieties, the interfacial resistance at the metal-ligand interface is markedly reduced, leading to the emergence of unprecedented optical and electronic properties (Hu et al. 2016a).

Isonitrile, the isomer of nitrile with an isomerization energy of 173 kJ/mol, has two resonant structures, one with a triple bond between C and N and the other a double bond with a strong carbenic character (Ramozzi et al. 2012), $R{-}N^+{\equiv}C^- \leftrightarrow R{-}N{=}C{:}$, and thus may adsorb onto transition-metal surfaces. For instance, it has been reported that isonitrile binds strongly on Ni(100) (Friend et al. 1981b), and Ni(111) (Friend et al. 1981a; Hemminger et al. 1979) surfaces with the N≡C bond lying parallel to the metal surface. On Rh(111) (Semancik et al. 1983), isonitrile adsorbs to the surface in parallel at lower coverages and upright at higher coverages. However, isonitrile adopts only the vertical structure on supported Rh/A1$_2$O$_3$ (Cavanagh and Yates 1981), and on Pt(111) metal surfaces in an upright structure with the terminal carbon bonded to two Pt atoms (Avery et al. 1985). Isonitrile binds to Ag (311) surface in a tilted or lying-down geometry at low coverages, whereas only upright bonding is observed at higher coverages (Ceyer and Yates 1985). On powdered Au (Robertson and Angelici 1994), isonitrile is bound weakly to the metal in a linear structure with the terminal carbon bonded to one metal atom. Kim et al. studied the adsorption characteristics of isonitrile molecules on various noble metal surfaces, such as Pd, Pt, and Au, by using surface-enhanced Raman scattering (SERS) and proposed that interfacial bonding modes

might entail on-top, 2-fold bridge, and 3-fold hollow sites.(Kim et al. 2010, 2011; Kim and Kim 2006) They reported that aryl isonitriles adsorbed on Au and Pt by forming exclusively metal−C≡N bonds, via a pure σ type interaction in the case of gold, as compared with a σ/π synergistic interaction on Pt. In these earlier studies, the adsorption dynamics of isonitrile were examined mostly on bulk metal surfaces. In another study, Schiffrin and co-workers reported the preparation of Pt nanoparticles passivated with alkyl isonitriles (Horswell et al. 1999). It was found that the C≡N vibrational energy blue-shifted by more than 70 cm^{-1} upon adsorption on Pt nanoparticles, due to increased electron donation from N to the terminal C through the σ/π bond. Yet, the bonding nature of the metal-ligand interfacial linkage has remained largely unexplored. Due to the carbenic nature of the isonitrile moiety, it is possible that isonitrile may form metal=C=N− π bond on metal surfaces. This is the primary motivation of the present study.

Herein, stable ruthenium nanoparticles were prepared by the self-assembly of isonitrile ligands on "bare" ruthenium colloid surfaces. ^{1}H NMR and FTIR characterizations, as well as metathesis reaction with vinyl derivatives suggested that the isonitrile ligands adsorbed to the Ru nanoparticle surface in an upright structure forming Ru=C=N−R interfacial linkages. This work not only unraveled the bonding nature of isonitrile on ruthenium metal surfaces, but also provided a novel and feasible approach for the formation of ruthenium-carbene (Ru=Carbene) double bond from stable and commercially available isonitrile molecules, which would rather be more cost-effective than from diazomethane (Chen et al. 2006) or stable N-heterocyclic carbenes (Crudden et al. 2014, 2016; Zhukhovitskiy et al. 2013).

Experimental section

Chemicals

Ruthenium chloride (RuCl$_3$, 99%, ACROS), 1,2-propanediol (99%+, ACROS), sodium acetate (NaOAc•3H$_2$O, 99.5%, ACROS), 1-aminopyrene (99%, TCI), 4-hexylaniline (> 98%, TCI), sodium acetate (NaOAc, ACROS), potassium hydroxide (KOH, ACROS), and magnesium sulfate (MgSO$_4$, ACROS) were used as received. All solvents were obtained from typical commercial sources at their highest purity and

used without further treatment. Water was supplied by a Barnstead Nanopure water system (18.2 MΩ cm).

Synthesis of 1-vinylpyrene (VPy), 1-isocyanopyrene (CNPy), 1-hexyl-4-isocyanobenzene (CNBH) and dodecyl isonitrile (CNC12)

The synthesis of VPy has been described previously (Chen et al. 2009). CNPy was prepared by following a previous procedure (Ugi et al. 1965; Weber and Gokel 1972). Briefly, KOH (15.6 mmol, 875.31 mg) was added into 30 mL of methanol in a 100-mL round-bottom flask under magnetic stirring. 1-Aminopyrene (5.2 mmol, 1.129 g) was then added into the above solution, followed by the dropwise addition of 10 mL of chloroform. The reaction was run for 6 h and monitored by TLC. After the white precipitate was removed by filtration, the remaining solution was collected and purified by column chromatography with silica gel (EtOAc–hexane) to yield CNPy.

CNBH and CNC12 were prepared by following the same procedure except that 1-aminopyrene was replaced with an equivalent amount of 4-hexylaniline and 1-dodecylamine.

Preparation of ruthenium nanoparticles

The synthetic procedure of organically capped ruthenium nanoparticles involved the preparation of "bare" ruthenium colloids by thermolysis of $RuCl_3$ in 1,2-propanediol and self-assembly of organic ligands on the ruthenium nanoparticle surface, as detailed previously (Kang and Chen 2012). To prepare CNBH-capped ruthenium (RuCNBH) nanoparticles, 0.28 mmol of $RuCl_3$ and 2 mmol of NaOAc were co-dissolved in 100 mL of 1,2-propanediol, and the solution was heated to 165 °C and thermally refluxed for 30 min under vigorous stirring. The appearance of a dark-brown solution signified the formation of ruthenium nanoparticles passivated by sodium acetate. The average diameter of the nanoparticles was 2.07 ± 0.46 nm, as determined by TEM measurements (Fig. S1). Once the ruthenium nanoparticle solution was cooled down to room temperature, 0.84 mmol of CNBH in 50 mL of toluene was

added into the solution. After vigorous mixing for 3 h, the dark brown color was transferred from 1,2-propanediol to toluene, indicating successful passivation of the ruthenium nanoparticles with the added CNBH ligands. The toluene phase was then collected and the solvents were removed by rotary evaporation. The solids were rinsed with a copious amount of methanol to remove excess ligands. The resulting nanoparticles were denoted as RuCNBH, which might be readily dispersed in nonpolar solvents such as toluene, tetrahydrofuran, chloroform, dichloromethane, etc. The synthetic procedure was summarized in Scheme 1.

CNC12-capped ruthenium (RuCNC12) nanoparticles were prepared in the same fashion except that an equivalent amount of CNC12 was used instead of CNBH. Similarly, another sample was prepared by adding a mixture of 0.28 mmol of CNPy and 0.56 mmol of CNBH (0.84 mmol in total), affording nanoparticles capped with a mixed monolayer of CNPy and CNBH, which were referred to as RuCNPy. The coverage of the CNPy moieties on the RuCNPy nanoparticles surface was estimated to be 22.7% (Fig. S2).

Pyrene-functionalized nanoparticles were also prepared by olefin metathesis reactions of RuCNBH nanoparticles with VPy. Experimentally, a calculated amount of RuCNBH and VPy was codissolved in toluene under magnetic stirring for 1 d. The nanoparticles were precipitated by adding methanol into the solution and collected by centrifugation. This process was repeated multiple times to remove excess VPy and displaced CNBH ligands, affording purified nanoparticles which were referred to as RuVPy. The coverage of the VPy moieties on the RuVPy nanoparticles surface was estimated to be 20.4% (Fig. S3).

Characterization

^{1}H NMR spectroscopic measurements were carried out by using concentrated solutions of the nanoparticles in CD_2Cl_2 or $CDCl_3$ with a Bruker 400 MHz NMR spectrometer. FTIR measurements were carried out with a Nicolet FTIR spectrometer. The samples were prepared by dropcasting the particle solutions onto a KBr disk and dried by a N_2 gas flow. Photoluminescence
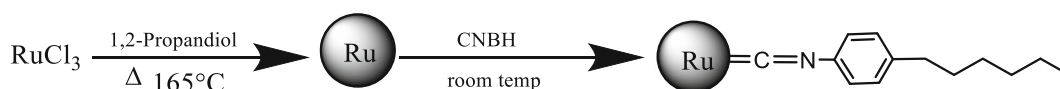
Scheme 1 Schematic of the synthesis of RuCNBH nanoparticles

excitation, emission, and time-resolved decay measurements were conducted with a Horiba QM3400 spectrometer. X-ray photoelectron spectroscopic (XPS) were measured on a Thermo Escalab 250Xi instrument.

Results and discussion

The structures of the samples were first characterized by NMR measurements. Fig. 1a displays the ^{1}H NMR spectrum of CNBH ligands, where four sharp peaks can be found at 0.89, 1.20, 2.6, and 7.30 ppm, due to the terminal methyl, methylene, α–CH_2 next to the phenyl ring, and phenyl protons, respectively. These four peaks were also observed with the RuCNBH nanoparticles in curve (B) but significantly broadened, and the phenyl protons were markedly down-shifted to ca. 7.00 ppm. Note that broadening of NMR spectral features for nanoparticles, in comparison to those of the monomeric ligands, has been observed extensively and ascribed to the slowed tumbling of the nanoparticles and diverse binding sites on the nanoparticles surfaces, such as vertices, edges, terraces, etc., and may be exploited as an effective measure of the purity of the nanoparticle samples.(Chen et al. 2006; Hostetler et al. 1998) As mentioned earlier, alkyl isonitrile displays an almost linear molecular structure with two resonant structures, one with a triple bond between C and N (R—N^+≡C^-) and the other a double bond with a significant carbenic character (R—N=C:) (Ramozzi et al. 2012), which may be

exploited for the chemical functionalization of metal surfaces. In such a case, the N atom gains π lone pair electrons from the C≡N triple bond and changes its hybridization from sp. to sp^2 with the charge state changed from positive to neutral. Therefore, the decrease of the chemical shift of the phenyl protons from 7.30 ppm for CNBH monomer to 7.00 ppm for the RuCNBH nanoparticles might be ascribed to the lower electron withdrawing capability of the neutral N in Ru=C=N– than that in isonitrile monomers (C^-≡N^+–R). One may argue that the charge state of N in isonitrile might also be reduced by taking the side-on adsorption mode, where N directly interacts with Ru metal. However, in such an interfacial configuration, the phenyl ring would also be lying flat on the nanoparticle surface. The resulting loose packing of the surface ligands is unlikely to stabilize the nanoparticles, contradicting experimental observations that the nanoparticles might be collected from solution and redispersed in common organic solvents. In addition, as depicted in Fig. 1b, the phenyl protons of the CNBH ligands on the nanoparticles remained clearly defined (though markedly broadened), indicating that the phenyl ring was unlikely on the metal core surface. Similar behaviors were observed with RuCNC12 nanoparticles (Fig. S4). In the side-on mode, the α–H protons of the CNC12 ligands would be too close to the Ru nanoparticle surface and broadened into baseline. However, the α–H protons were clearly observed at 3.2 ppm, in comparison with 3.4 ppm for CNC12 free ligands (Fig. S4), indicating that isonitrile molecules most

Fig. 1 ^{1}H NMR spectra of (A) CNBH and (B) RuCNBH nanoparticles in CD$_2$Cl$_2$
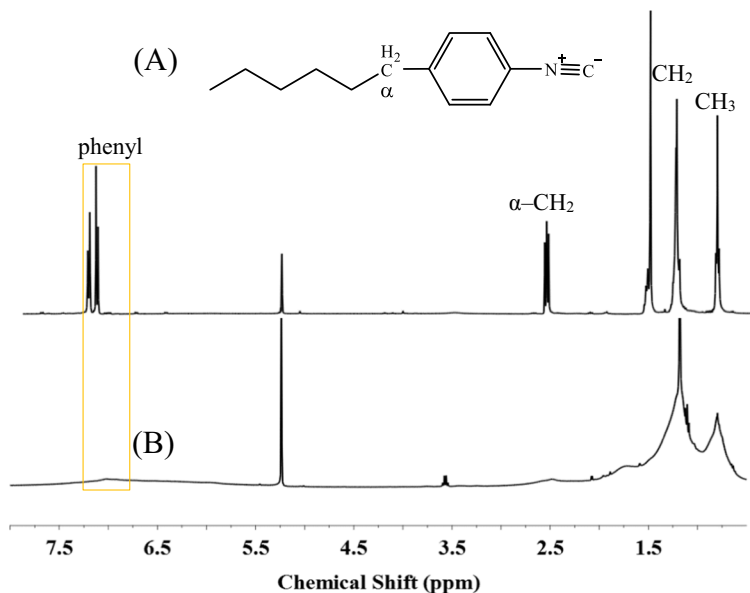
likely adopted an end-on configuration, instead of the side-one mode and direct N bonding with Ru nanoparticle surface. The formation of Ru=C=N– was further corroborated by olefin metathesis reactions with vinyl derivatives (vide infra).

The structures of the RuCNBH nanoparticles were then examined by XPS measurements. Figure 2 depicts the high-resolution XPS scans of the (A) Ru 3d and C 1s and (B) N 1s electrons of RuCNBH nanoparticles. Deconvolution of the spectrum in panel (A) yields four subpeaks at 280.7, 284.3, 284.8, and 285.0 eV. The pair at 284.3 eV (pink) and 285.0 (cyan) might be ascribed to the sp^2 and sp^3 carbons in the CNBH ligands(Rybachuk and Bell 2009; Zhang et al. 2007). It should be noted that no sp. hybridized C 1s were resolved, consistent with the conversion of C_{sp} in $C^-\equiv N^+$– to C_{sp2} in Ru=C=N–. The other pair at 280.7 (dark yellow) and 284.8 eV (blue) are assigned to metallic Ru $3d_{5/2}$ and Ru $3d_{3/2}$ electrons, in good agreement with results of our earlier studies of nitrile-capped ruthenium nanoparticles (Zhang et al. 2017). The positive shift of ca. 0.5 eV, relative to those of bulk metallic ruthenium, is most likely due to back donation of the Ru-d electrons to the π* orbital of the CNBH ligands forming Ru=C=N– interfacial bonds.

For the N 1s spectrum in panel (B), the N 1s binding energy can be estimated to be 398.4 eV for the RuCNBH nanoparticles, a red shift of 1.4 eV as compared to that of phenyl isonitrile monomers which has been reported to be 399.8 eV due to the positively charged N atom.(Pranger et al. 2005; Sohn and White 2007) This discrepancy may be attributed to the change of charge state of the N atom in RuCNBH due to the formation of Ru=C=N– interfacial bonds, where the N gained a pair of electrons and became neutral. This is actually in good agreement with results reported in the literature, where the binding energy of N 1s in isonitrile has been found to shift to 398.5 and 397.8 eV upon adsorption onto Pd and Cu(111) surfaces, respectively (Stapleton et al. 2005).

Further, structural insights into the interfacial linkage of the RuCNBH nanoparticles were obtained by FTIR studies. From Fig. 3, one can see that CNBH monomers exhibited a series of well-defined vibrational bands, including the phenyl C–H vibration at 3032 cm^{-1} and C=C at 1661 cm^{-1}, and terminal isonitrile (−N≡C) stretch at 2119 cm^{-1}. Interestingly, the sharp band of –N≡C vanished for the RuCNBH nanoparticles, and concurrently, three new bands appeared at 2115, 2043, and 1944 cm^{-1}. In prior studies of isonitrile adsorption on laser-ablated Pt nanoaggregates (Kim et al. 2011), three vibrational bands were also observed at 2166, 2124, and 1997 cm^{-1}, and attributed to the N≡C triple bond of isonitriles bound onto the on-top, 2-fold bridge and 3-fold hollow sites, respectively, of the Pt nanoaggregates, and the redshift of the frequency was ascribed to the back donation of Pt d electrons to the π* orbital of the N≡C moiety. However, the carbenic nature of the isonitrile moiety and the possibility of the formation of Pt=C=N– linkages was neglected. Note that when acetylene derivatives (−C≡CH) were self-assembled onto ruthenium nanoparticles forming ruthenium-vinylidene (Ru=C=CH−) interfacial bonds, three vibrational bands at similar positions were also observed, with a marked redshift of the vibrational energies as compared to that
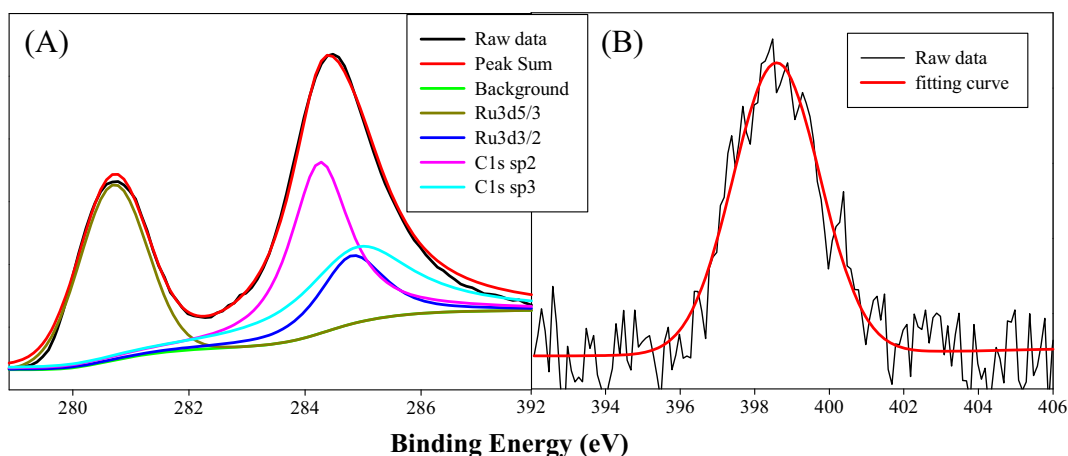
Fig. 2 High-resolution XPS scans of the **a** Ru 3d and C1s and **b** N 1s electrons of RuCNBH nanoparticles. Black curves are experimental data and colored curves are deconvolution fits

Fig. 3 FTIR spectra of CNBH monomers and RuCNBH nanoparticles. Inset shows the zoom-in for the Ru=C=N stretching modes at 2115, 2043, and 1944 cm^{-1}
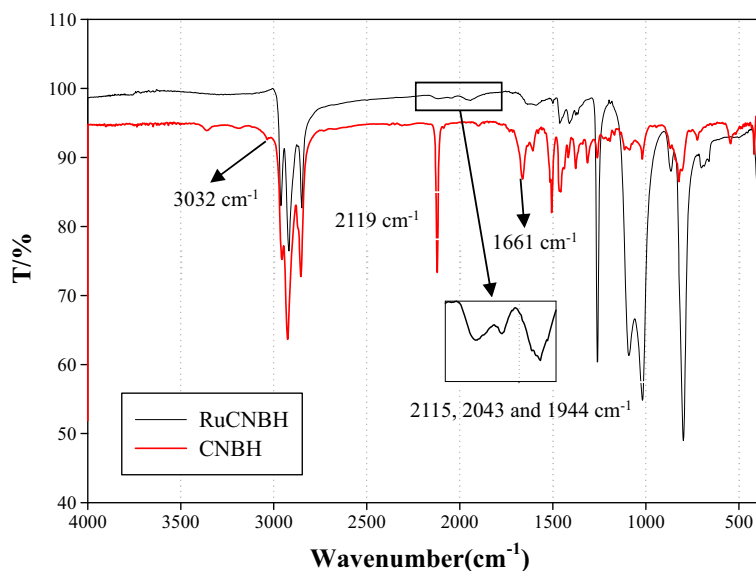
of the free ligands (Kang et al. 2012b). Thus, it is likely that when isonitrile ligands adsorbed onto ruthenium nanoparticle surface, a similar interfacial linkage involving Ru=C=N− was formed instead of Ru−C≡N−, where the Ru=C conjugated linkage markedly enhanced the vibrational energy of the adjacent C=N, as observed in earlier reports (Horswell et al. 1999; Hu et al. 2016b). For example, the C=C double bond is generally found at 1650 cm^{-1} for alkene, but at 1957 cm^{-1} for allene (C=C=C) (Horswell et al. 1999), and even higher at 2047 cm^{-1} for Pt=C=C (Hu et al. 2016b). One may also note that the three vibrational bands for isonitrile on Ru

nanoparticle surfaces are about 50 cm^{-1} lower than those on Pt, possibly due to the stronger back donation of Ru than Pt. Note that the work functions of Pt and Ru are 5.65 and 4.71 eV (Drummond 1999), respectively. This means that the Fermi level of Ru is 0.94 eV higher than that of Pt, leading to stronger back donation by the Ru d electrons than by Pt to the C=N π* orbital and more redshift of the vibrational bands in FTIR measurements.

The formation of Ru=C=N conjugated linkages on RuCNHB nanoparticle surface was further confirmed by successful olefin metathesis reaction with olefin

Fig. 4 Excitation and emission spectra of VPy monomers (46.6 μM), and RuVPy (0.1 mg/mL) in CHCl$_3$
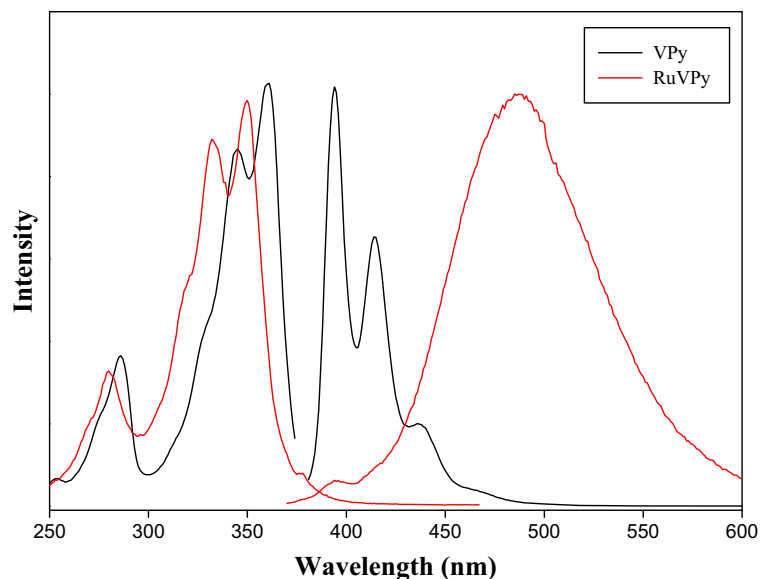
derivatives such as VPy (Chen et al. 2006; Hu et al. 2016b; Rybachuk and Bell 2009). Figure 4 displays the photoluminescence excitation and emission spectra of the resulting RuVPy nanoparticles, where the excitation features were very analogous to those of the VPy monomers but the emission maximum exhibited a marked red shift from 380 to 487 nm. Similar behaviors have also been observed in earlier studies where acetylene-stabilized ruthenium nanoparticles were used instead for metathesis reactions with VPy (Kang et al. 2012b; Rybachuk and Bell 2009), further corroborating the formation of Ru=C=N interfacial linkages on RuCNBH nanoparticle surface. Such conjugated interfacial bonds led to apparent intraparticle charge delocalization between the particle-bound pyrene moieties, and the nanoparticle photoluminescence characteristics became analogous to those of pyrene dimers (Kang et al. 2012b; Rybachuk and Bell 2009).

Charge delocalization through the conjugated Ru=C=N– interfacial bonds was also manifested with the RuCNPy nanoparticles that were capped with a mixed monolayer of CNBH and CNPy (Fig. 5). Through the Ru metal core and conjugated Ru=C=N–π bonds, the particle-bound pyrene moieties are anticipated to behave analogously to its dimers bridged with conjugated linkers, leading to a red shift of the emission band (Chen et al. 2009). Vice versa, such conjugation and charge delocalization could be manifested by the red shift of the photoemission spectra of the nanoparticle-bound pyrene moieties. Figure 5a depicts the excitation and emission spectra of CNPy monomers

and RuCNPy nanoparticles in $CHCl_3$. The latter exhibits an emission maximum at 407 nm, a red shift of 27 nm relative to that of the former, again, suggesting extensive conjugation through the interfacial π bonds on the RuCNPy nanoparticle surface. However, the red shift (27 nm) is drastically smaller than that (107 nm) observed above with the RuVPy nanoparticles, implying a weaker π character of the Ru=C=N−Py interfacial bond than that of Ru=C=N–.

The conjugated interfacial bond in RuCNPy was further explored by time-resolved photoluminescence measurements, as shown in Fig. 5b. The emission decay profiles were fitted by a single exponential function where the lifetimes were calculated to be 11 and 3 ns for CNPy monomers and RuCNPy nanoparticles, respectively. Compared to that of CNPy monomer, the lifetime of nanoparticles-bound CNPy moieties was remarkably reduced. The lifetime of the excited state of CNPy monomers was dominated by the charge transfer from the excited state to the ground state. However, the excited state of CNPy moieties bound on Ru metal cores could also decay by electron transfer through Ru=C=N to Ru metal core as a second channel. Thus, the decreased lifetime for RuCNPy, as compared to that of PyNC monomers, was likely due to the enhanced electron transfer from the pyrene moieties to the Ru metal cores (Chen et al. 2009), where the conjugated Ru=C=N interfacial bonds facilitated the ligand-to-metal charge transfers (LMCT) (Berezin and Achilefu 2010) and thus reduced the lifetime of the excited state. This is in agreement with results from prior studies with
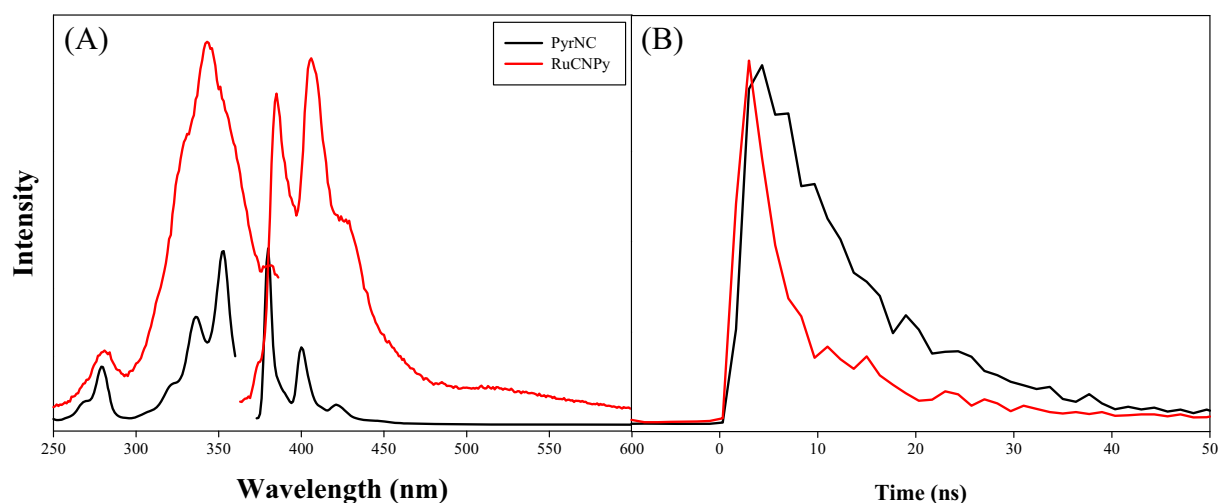
Fig. 5 **a** Excitation and emission spectra and **b** time-resolved fluorescence decay dynamics of CNPy monomers and RuCNPy nanoparticles in chloroform

olefin-capped ruthenium nanoparticles, further supporting the interfacial charge transfer through Ru=C=N bonds (Chen et al. 2009).

Conclusion

In summary, stable ruthenium nanoparticles were prepared by the self-assembly of isonitrile ligands onto "bare" ruthenium colloid surfaces forming Ru=C=N interfacial bonds, which were characterized by ^{1}H NMR, FTIR, and XPS measurements. This was further confirmed by successful olefin metathesis reaction with vinyl derivatives, which suggests an end-on configuration of the isonitrile ligands on the Ru nanoparticle surface. The conjugated Ru=C=N interfacial bonding linkage led to extensive intraparticle charge delocalization and hence strong conjugation between particle-bound organic functional moieties, as manifested by a red shift of the emission maximum and reduced lifetime of nanoparticle-bound pyrene as compared to results of the free monomers. These results further underline the fundamental importance of metal–organic contacts in the manipulation of interfacial charge transfer, which is a critical and yet unresolved research topic in molecular devices.

Compliance with ethical standards

Conflict of interest   The authors declare that they have no conflict of interest.

References

Avery N, Matheson T, Sexton B (1985) Bonding configurations of the isoelectronic molecules, CO, CH3NC and CH3CN on Pt (111). Appl Surf Sci 22:384–391

Berezin MY, Achilefu S (2010) Fluorescence lifetime measurements and biological imaging. Chem Rev 110:2641–2684

Cavanagh R, Yates J Jr (1981) Surface binding of an electronic analog to CO: infrared evidence for CH3NC chemisorption on Rh/Al2O3. J Chem Phys 75:1551–1559

Ceyer S, Yates J Jr (1985) Orientation of methyl isocyanide adsorbed on silver (311). J Phys Chem 89:3842–3845

Chen SW et al (1998) Gold nanoelectrodes of varied size: transition to molecule-like charging. Science 280:2098–2101. https://doi.org/10.1126/science.280.5372.2098

Chen W, Davies JR, Ghosh D, Tong MC, Konopelski JP, Chen SW (2006) Carbene-functionalized ruthenium nanoparticles. Chem Mater 18:5253–5259. https://doi.org/10.1021/cm0615951

Chen W, Zuckerman NB, Lewis JW, Konopelski JP, Chen S (2009) Pyrene-functionalized ruthenium nanoparticles: novel fluorescence characteristics from intraparticle extended conjugation. J Phys Chem C 113:16988–16995. https://doi.org/10.1021/jp906874f

Crudden CM et al (2014) Ultra stable self-assembled monolayers of N-heterocyclic carbenes on gold. Nat Chem 6:409–414. https://doi.org/10.1038/nchem.1891

Crudden CM et al (2016) Simple direct formation of self-assembled N-heterocyclic carbene monolayers on gold and their application in biosensing. Nat Commun 7:12654. https://doi.org/10.1038/Ncomms12654

Drummond JT (1999) Work functions of the transition metals and metal silicides. Sandia National Laboratories, US (internal report)

Friend C, Muetterties E, Gland J (1981a) Vibrational studies of acetonitrile and methyl isocyanide adsorbed on nickel (111) and nickel (111)-carbon surfaces. J Phys Chem 85:3256–3262

Friend C, Stein J, Muetterties E (1981b) Coordination chemistry of metal surfaces. 2. Chemistry of CH/sub 3/CN and CH/sub 3/NC on nickel surfaces. J Am Chem Soc 103:767–772

Hemminger J, Muetterties E, Somorjai G (1979) Coordination chemistry study of a nickel surface. The chemistry of Ni (111) with triply bonded molecules. J Am Chem Soc 101:62–67

Horswell SL, Kiely CJ, O'Neil IA, Schiffrin DJ (1999) Alkyl isocyanide-derivatized platinum nanoparticles. J Am Chem Soc 121:5573–5574. https://doi.org/10.1021/Ja984284n

Hostetler MJ et al (1998) Alkanethiolate gold cluster molecules with core diameters from 1.5 to 5.2 nm: core and monolayer properties as a function of core size. Langmuir 14:17–30. https://doi.org/10.1021/La970588w

Hu P, Chen L, Kang X, Chen S (2016a) Surface Functionalization of Metal Nanoparticles by Conjugated Metal-Ligand Interfacial Bonds: Impacts on Intraparticle Charge Transfer. Acc Chem Res 49:2251–2260. https://doi.org/10.1021/acs.accounts.6b00377

Hu PG, Chen LM, Deming CP, Bonny LW, Lee HW, Chen SW (2016b) Identification of the formation of metal-vinylidene interfacial bonds of alkyne-capped platinum nanoparticles by isotopic labeling. Chem Commun 52:11631–11633. https://doi.org/10.1039/c6cc05626a

Kang X, Chen S (2012) Electronic conductivity of alkyne-capped ruthenium nanoparticles. Nanoscale 4:4183–4189. https://doi.org/10.1039/c2nr30213f

Kang X, Zuckerman NB, Konopelski JP, Chen S (2010) Alkyne-stabilized ruthenium nanoparticles: manipulation of intraparticle charge delocalization by nanoparticle charge states. Angew Chem 49:9496–9499. https://doi.org/10.1002/anie.201004967

Kang X, Song Y, Chen S (2012a) Nitrene-functionalized ruthenium nanoparticles. J Mater Chem 22:19250–19256. https://doi.org/10.1039/c2jm33783e

Kang X, Zuckerman NB, Konopelski JP, Chen S (2012b) Alkyne-functionalized ruthenium nanoparticles: ruthenium-vinylidene bonds at the metal-ligand interface. J Am Chem Soc 134:1412–1415. https://doi.org/10.1021/ja209568v

Kim NH, Kim K (2006) Adsorption characteristics of arylisocyanide on Au and Pt electrode surfaces: surface-enhanced Raman scattering study. J Phys Chem B 110: 1837–1842. https://doi.org/10.1021/jp055541v

Kim K, Kim KL, Choi JY, Lee HB, Shin KS (2010) Surface enrichment of Ag atoms in Au/Ag alloy nanoparticles revealed by surface-enhanced Raman scattering of 2,6-dimethylphenyl isocyanide. J Phys Chem C 114:3448–3453. https://doi.org/10.1021/jp9112624

Kim K, Kim KL, Choi JY, Shin KS (2011) Effect of organic vapors and potential-dependent Raman scattering of 2,6-dimethylphenylisocyanide on platinum nanoaggregates. Phys Chem Chem Phys 13:5981–5986. https://doi.org/10.1039/c0cp01619e

Lu Y, Chen W (2012) Sub-nanometre sized metal clusters: from synthetic challenges to the unique property discoveries. Chem Soc Rev 41:3594–3623. https://doi.org/10.1039/c2cs15325d

Pranger L, Goldstein A, Tannenbaum R (2005) Competitive self-assembly of symmetrical, difunctional molecules on ambient copper surfaces. Langmuir 21:5396–5404. https://doi.org/10.1021/la050508l

Ramozzi R, Chéron N, Braïda B, Hiberty PC, Fleurat-Lessard P (2012) A valence bond view of isocyanides' electronic structure. New J Chem 36:1137–1140

Robertson MJ, Angelici RJ (1994) Adsorption of aryl and alkyl isocyanides on powdered gold. Langmuir 10:1488–1492

Rybachuk M, Bell JM (2009) Electronic states of trans-polyacetylene, poly(p-phenylene vinylene) and sp-hybridised carbon species in amorphous hydrogenated carbon probed by resonant Raman scattering. Carbon 47:2481–2490. https://doi.org/10.1016/j.carbon.2009.04.049

Semancik S, Haller GL, Yates JT (1983) The adsorption and dissociation of methyl isocyanide on Rh(111). J Chem Phys 78:6970–6981. https://doi.org/10.1063/1.444645

Sohn Y, White JM (2007) Phenyl isocyanide on Cu(111): bonding and interfacial energy level alignment. J Phys Chem C 111: 7816–7825. https://doi.org/10.1021/jp070903f

Stapleton JJ, Daniel TA, Uppili S, Cabarcos OM, Naciri J, Shashidhar R, Allara DL (2005) Self-assembly, characterization, and chemical stability of isocyanide-bound molecular wire monolayers on gold and palladium surfaces. Langmuir 21:11061–11070. https://doi.org/10.1021/la051094z

Ugi I, Fetzer U, Eholzer U, Knupfer H, Offermann K (1965) Isonitrile syntheses. Angew Chem Int Ed Engl 4:472–484

Weber WP, Gokel GW (1972) An improved procedure for the Hofmann carbylamine synthesis of isonitriles. Tetrahedron Lett 13:1637–1640

Zhang S, Chandra KL, Gorman CB (2007) Self-assembled monolayers of terminal alkynes on gold. J Am Chem Soc 129: 4876. https://doi.org/10.1021/ja0704380

Zhang F, Huang L, Zou J, Yan J, Zhu J, Kang X, Chen S (2017) Nitrile-functionalized ruthenium nanoparticles: charge delocalization through Ru − N ≡ C interface. J Nanopart Res 19: 106. https://doi.org/10.1007/s11051-017-3801-2

Zhukhovitskiy AV, Mavros MG, Van Voorhis T, Johnson JA (2013) Addressable carbene anchors for gold surfaces. J Am Chem Soc 135:7418–7421. https://doi.org/10.1021/ja401965d